

# BUNCHING AND FOCUSING OF AN INTENSE ION BEAM FOR TARGET HEATING EXPERIMENTS\*

J.E. Coleman, D. Ogata, Dpt. of Nuclear Engineering, UC Berkeley, Berkeley, CA 94720, USA.  
 P.A. Seidl, P.K. Roy, LBNL, Berkeley, CA 94720, USA.  
 E.P. Gilson, A.B. Sefkow, PPPL, New Jersey 08543, USA.  
 D.R. Welch, Voss Scientific, Albuquerque, NM 87108, USA.

## Abstract

An experiment to focus transversely and simultaneously axially bunch a space charge neutralized  $K^+$  ion beam has been carried out at LBNL. The principal objectives of the simultaneous bunching and focusing experiments are to control the beam envelope, demonstrate effective neutralization of the beam space-charge, control the velocity tilt on beam, understand effects of net defocusing, field imperfections, limitations on minimal spot size such as emittance and aberrations and to quantify the longitudinal phase space. A demonstration of increased axial compression and a reduction in spot size compared to earlier measurements is presented.

## INTRODUCTION

Future warm dense matter (WDM) experiments with space-charge dominated ion beams require simultaneous longitudinal bunching and transverse focusing [1]. Given the existing ion source and injector beam current capabilities, the required beam manipulations are to longitudinally bunch the beam two orders of magnitude to a pulse length shorter than the target disassembly time and to focus the beam transversely to a sub-mm radius. The space charge of the beam must be neutralized so only emittance limits the final beam density. In order to axially compress a charged beam bunch a head to tail velocity ramp must be applied and a low beam temperature must be maintained.

The Neutralized Drift Compression Experimental (NDCX) campaign is exploring the physical limits on compression and focusing of ion beams for heating material to WDM and fusion ignition conditions [2]. On

the NDCX an induction bunching module (IBM) provides a velocity ramp. As a result undesired radial electric fields are generated in the gap across which the IBM voltage is applied that include a net radial defocusing effect to the bunching beam. Following analysis of the effect [3] it was determined that tuning the initial beam envelope to compensate for the defocusing of the IBM enables simultaneous focusing.

## SIMULTANEOUS FOCUSING EXPERIMENT

Studies of combined transverse and longitudinal focusing of 0.3-MeV, 26-mA singly charged  $K^+$  ion beam were conducted on the NDCX as shown in Fig. 1. The IBM was located downstream of a beam diagnostic box located at the exit of the 4-solenoid lattice [4]. The 4-solenoid transport lattice was used to match the beam to the desired envelope parameters ( $a = 15$  mm,  $a' = -30$  mrad) at the entrance to the IBM. The IBM provided a linear velocity ramp ( $\Delta v/v \approx \pm 15\%$ ) on a 200 ns portion of the injected beam and was tuned specifically for the beam energy and a drift distance of 1.29 m. Plasma neutralization began 28 cm downstream with an 85-cm long ferro-electric plasma column (FEPS) [5]. The fully neutralized beam then drifted 16 cm to the focal plane. A filtered cathodic arc plasma source (FCAPS) was also used for neutralizing the beam at the diagnostic plane [6].

The IBM was tuned to best match the ideal velocity tilt (Fig. 2). Slight improvements have been made in the resulting waveform although identical hardware was used

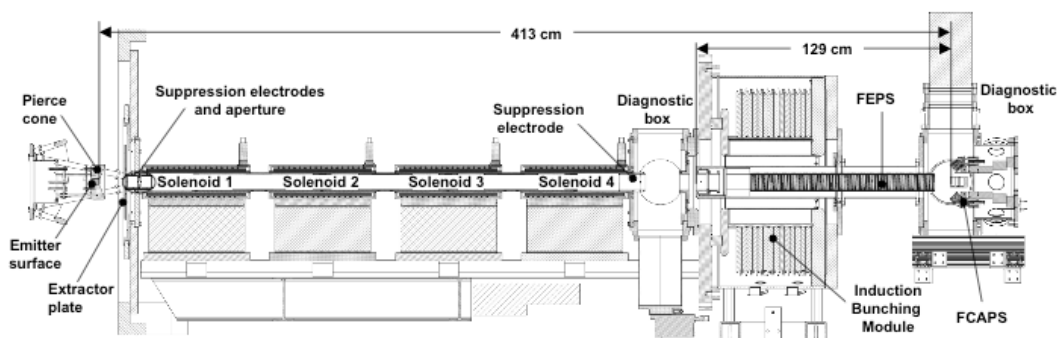


Figure 1: Elevation view of the Simultaneous Focusing Experiment on NDCX.

\*Work supported by US DOE under Contract No. DE-AC02-05H11231 and DE-AC02-76CH3073 for HIFS-VNL.

for the IBM in recent experiments compared to that reported by Roy et al., in 2005 [7]. Examining the voltage difference from the ideal case over the relevant portion of the injected waveform ( $0.1 < t < 0.25 \mu\text{s}$ ) shows that the new waveform has an average voltage difference of  $< 0.5 \text{ kV}$  compared to  $> 1.5 \text{ kV}$  in 2005 [Fig. 2(b)].

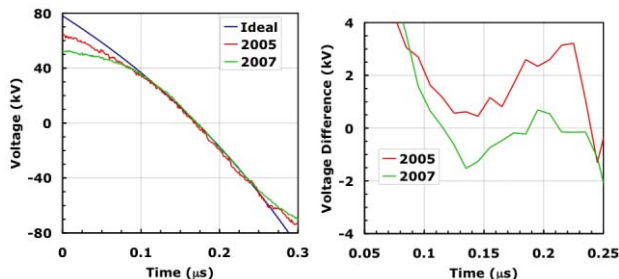


Figure 2: (a) IBM waveform comparison to ideal case for 2005 and 2007; (b) improvement in voltage difference (filtered for clarity).

The aforementioned defocusing effect was quantified and compensated for with a tune [Fig. 3(a)] where the beam envelope expands to about 30 mm in the fourth transport solenoid [Fig. 3(b)]. The maximum excursion of the real beam was limited by beam halo, centroid offsets, the beam pipe radius (43 mm), and the radius of the in-bore diagnostic at the exit of the fourth solenoid (37 mm). Beam space charge and the radial defocusing effects provided by the velocity tilt required this steep convergence angle. Plasma neutralization did not start until 28 cm downstream of the induction gap causing the beam to lose most of its convergence due to space charge. Given all of these constraints a  $2\sigma_{\text{rms}}$  radius ( $a = 2^{1/2} \langle r^2 \rangle^{1/2}$ ) not much less than 5-mm was expected with sufficient plasma neutralization.

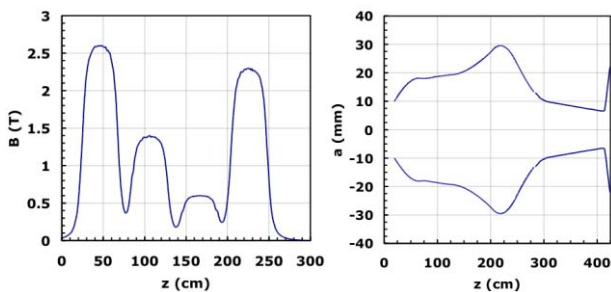


Figure 3: (a) Focusing lattice used to control; (b) the ideal beam envelope.

Although the transport solenoids and velocity tilt waveform had been tuned for a 300 kV  $\text{K}^+$  ion bunch with a focal length of 1.29 m it was expected that the beam envelope in the experiment might deviate by a few percent from the ideal calculation. There are two critical parameters for optimizing the envelope in the experiment. The first is the extraction voltage in the diode. Since, we have a constant perveance beam we can change the longitudinal envelope angle  $[z' = z \text{ (bunch length before axial compression)} / f \text{ (focal length)}]$  by less than 1 mrad by varying the beam energy by just 1 keV. In order to

maintain a constant beam envelope the field strength of the transport solenoids must be scaled by  $E^{1/2}$  ( $E$  is the beam energy). Once the operating points are determined for the axial focus, the transverse focus can be decoupled and optimized. Changes of just 0.02 T on a 2 T field make less than 1 mrad changes in the transverse envelope angle; although this is small, the drift length of 1.65 m after the fourth transport solenoid acts as a long lever arm.

Measurements were made to determine the axial focus. Several data sets demonstrate the dependence of the axial focal plane on  $E$  (Fig. 4). Two coupled parameters are quantified when measuring the axial focus; the compression ratio (ratio of axially compressed to uncompressed beam current) and the full width half maximum (FWHM) of the compressed pulse. The results of energy scans from 250-350 keV show the axial focus can be achieved with a  $E = 300 \text{ keV}$  however there is a variance of about 10% in the compression ratio and a fluctuation of less than 1 ns in the FWHM at the focus. This is could be contributed in part with voltage fluctuations of 5% and a timing jitter of 10 ns induced by the IBM.

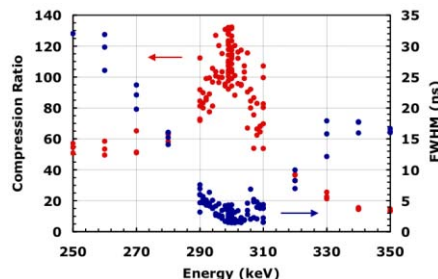


Figure 4: Energy dependence at the axial focal plane.

These recent experiments demonstrate good agreement between two different diagnostic techniques used to measure the axial focus of the ion beam. A pinhole Faraday cup with a 1 ns time response is used to measure the uncompressed and compressed beam current. Hole plates are used to screen out plasma electrons and ions from confounding the measurement of the beam current. A compressed pulse duration and compression ratio is also extracted from this measurement [8]. The second method uses a phototube with a sub-ns resolution to detect the beam-induced light emission from an intercepting alumina scintillator. This method can also measure the uncompressed and compressed light emission. However, the light collection efficiency and a low signal-to-noise ratio, make a compression ratio difficult to extract. Both methods have demonstrated compressed pulse widths of  $2.4 \pm 0.8 \text{ ns}$  at peak axial focus (Fig. 5). This pulse width corresponds to a compression ratio of greater than 100 (based on the fast Faraday cup), or a peak current  $> 2.6 \text{ A}$ ; an improvement from previous experiments [7]. Improvements in the velocity tilt (Fig. 2) and the use of the FEPS may help explain this. The FCAPS makes a high velocity plasma that might heat the beam when used beyond the focal plane (as was done in the past with a plasma guiding

magnetic field from a solenoid) reducing the peak axial focus.

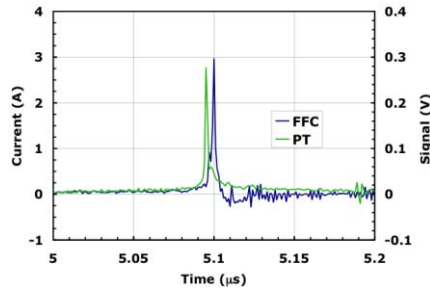


Figure 5. Current waveform at the focal plane for a neutralized  $K^+$  ion beam measured with the fast Faraday cup (FFC) (blue) and phototube (PT) (green).

After verifying the energy necessary to operate at axial focus, measurements were then made to establish that the time dependent transverse focal plane coincides with the axial focus. Measurements of the transverse beam distribution  $J(x,y)$  were made with a 100- $\mu\text{m}$  thick alumina scintillator and an image-intensified gated-CCD camera that imaged beam-induced light emission. The CCD was 512 x 512 pixels with a resolution of 18 pixels/mm. A 10 ns gate width was used to capture the beam distribution at axial compression ( $t = 5.095 \mu\text{s}$ ) (Fig. 6). Larger gate widths (100 ns) were used 100 and 200 ns before and after the simultaneously focused spot to keep a satisfactory signal-to-noise ratio.

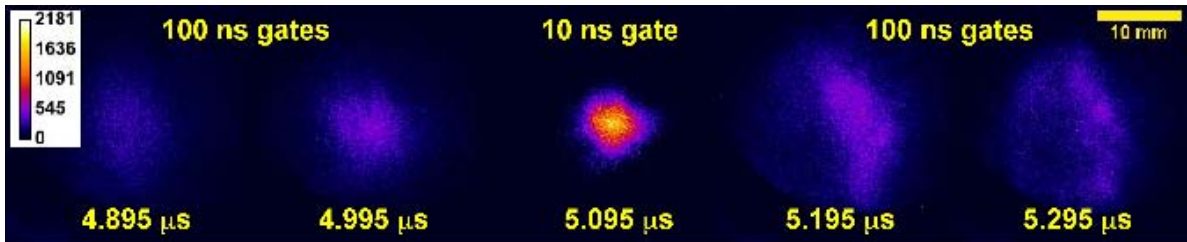


Figure 6: Time dependent transverse beam distributions demonstrating the simultaneous focal plane.

A nearly three-fold reduction in the spot size for the compressed pulse is shown in Fig. 7, where the horizontal and vertical  $2\sigma_{\text{rms}}$  radii ( $a$  and  $b$ ) have been extracted from the images of Fig. 6. Based on these measurements the beam density at the focal plane is in the range of  $10^{11} \text{ cm}^{-3}$ . Recent plasma density measurement verify that the plasma density should exceed the beam density throughout the drift compression section, and fully neutralize the beam space charge as it converges to the focal plane [9]. With these results the peak beam intensity is about  $2.3 \times 10^{-3} \text{ J/cm}^2$ .

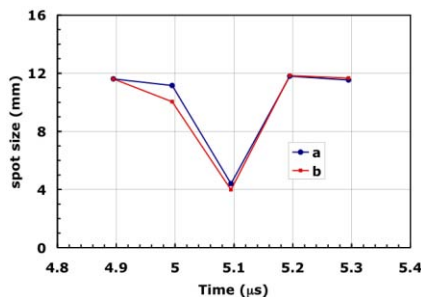


Figure 7: Projected spot radii ( $2\sigma_{\text{rms}}$ ) for distributions in Fig. 6.

## CONCLUSION

The addition of the FEPS along with improvements in the induction velocity tilt may help explain the improved axial focus ( $>100$  axial compression,  $< 2$  ns pulses). We have also successfully demonstrated a nearly three-fold reduction in spot size to demonstrate a simultaneously focused spot with  $a$  and  $b < 5$  mm. This is consistent with expectations from particle in cell simulations, though the

beam intensity is not yet what is desired for WDM experiments ( $\sim 1 \text{ J/cm}^2$ ) [1]. A further reduction in spot size, higher beam current and kinetic energy will increase the beam intensity required for the study of WDM.

## ACKNOWLEDGEMENT

We wish to thank Tak Katayanagi, Eugene Flor, Michael Dickinson, Cory Lee, Wayne Greenway, Matthaeus Leitner, Will Waldron, and Craig Rogers for their continued technical support.

## REFERENCES

- [1] J.J. Barnard et al., in Proceedings of the Particle Accelerator Conference, Knoxville, Tennessee, 2005, p. 2568, <http://www.JACoW.org/>.
- [2] P.A. Seidl et al., Nucl. Instrum. Meth. Phys. Res. A **577**, 215 (2007).
- [3] D.R. Welch et al., Nucl. Instrum. Meth. Phys. Res. A **577**, 231 (2007).
- [4] J.E. Coleman et al., "Electron cloud effects on an intense ion beam in a four solenoid lattice," to be submitted to Phys. Rev. ST Accel. Beams (2007).
- [5] P.C. Efthimion et al., Nucl. Instrum. Meth. Phys. Res. A **544**, 387 (2005).
- [6] A. Anders and G.Y. Yushkov, J. Appl. Phys. **91**, 4824 (2002).
- [7] P.K. Roy et al., Phys. Rev. Lett. **95** 234801 (2005).
- [8] A.B. Sefkow et al., Phys. Rev. ST Accel. Beams **9**, 052801(2006).
- [9] P.K. Roy et al., "A solenoid final focusing system with plasma neutralization for target heating experiments," these proceedings.